SANS Investigation and Conductivity of Pure and Salt-Containing Poly(bismethoxyphosphazene)

Y. Karatas,[†,§] W. Pyckhout-Hintzen,[‡] R. Zorn,[‡] D. Richter,[‡] and H.-D. Wiemhöfer*[,†]

Institut für Anorganische und Analytische Chemie, SFB 458, and International Graduate School of Chemistry (GSC-MS), Universität Münster, 48149 Münster, Germany, and Institut für Festkörperforschung, Forschungszentrum Jülich, 52425 Jülich, Germany

Received June 27, 2007; Revised Manuscript Received December 10, 2007

ABSTRACT: Poly(bismethoxyphosphazene) (PBMP) was synthesized, giving polymer melts with $T_g = -70.9$ °C. The chain dynamics of melts and DMF solutions of poly(bismethoxyphosphazene) (PBMP) was investigated by Small-Angle Neutron Scattering (SANS). The radius of gyration R_g was found as 144.7 ± 0.2 Å, and the average MW from SANS was 95000 Da. DMF revealed to be a good solvent for this polymer. From the scattering intensity of polymer solutions for high *q*-data, the slope was −1.647 in almost exact agreement with the expected excluded volume exponent by Flory which is $^5/_3$ affirming the good solvent property of DMF. GPC measurements of THF solutions were evaluated based on a universal calibration of polystyrene standards resulting in a rather similar value of 1.05×10^5 Da. Another series of SANS experiments was done with solutions of $LiSO_3CF_3$ (LiTf) in the title polymer. They also showed low T_g values down to −50 °C at 15 wt %. The SANS results (5 and 10 mol % LiTf as referred to the monomer units) showed almost no effect of the dissolved salt on the melt conformation of the polyphosphazene (almost random coil), and thus revealed a rather small interaction between salt and polymer. We also measured the ionic conductivity of salt-in-polymer systems with concentrations from 5 to 20 wt % LiTf. The room-temperature conductivity was 1.7×10^{-5} S/cm at 20 wt % LiTf and is thus rather high. The low interaction between salt and polymeric solvent is in agreement with the predominance of neutral ion pairs which is often observed in such polymer electrolytes.

1. Introduction

Polymers with inorganic backbone have attracted a growing interest during the last 20 years due to their superior chemical and physical properties. Among these inorganic polymers, polyphosphazenes with alternating phosphorus and nitrogen atoms along the chain and two organic groups attached at each phosphorus occupy a special position. They comprise by far the largest class of macromolecules with inorganic backbone, since a wide variety of side chains can be used to modify and fine-tune both the chemical and physical properties of these polymers.

As the research in this field has vastly expanded in the past decade, numerous reviews can be found with regard to the synthesis[1−3] and to potential applications of polyphosphazenes such as in fuel cells,[4−7] batteries,[8,9] biomedical applications,[10−16] membranes,[17−20] flame retardants,[21,22] etc. One of the promising applications of these inorganic polymers is their use as salt-in-polymer electrolytes, for instance as safe, ionically conducting membranes in lithium batteries.[23,24]

The common opinion in this area is that polymers with high segmental mobility and good coordination ability for heteroatoms, like oxygen or nitrogen, enhance the ionic motion of the mobile salt ions. Many different polymer structures have been synthesized and studied in the field of polyphosphazenes on the basis of this idea.[23,24] The polyphosphazene architecture which received most attention for polymer electrolyte applications up to now is poly[bis(methoxyethoxyethoxy)phosphazene] (MEEP). It was first synthesized and characterized by Allcock's group.[25−27] This polymer exhibits a room-temperature ionic conductivity of nearly 3×10^{-5} S cm^{-1}.[25,26] The methoxy-substituted derivative of polyphosphazene on the other hand was also synthesized before[28,29] but was not considered to be a candidate as a polymer electrolyte due to the presumably low concentration of coordinating heteroatoms.

The ionic conduction of polymeric electrolytes is assumed to take place predominantly in the amorphous region. On the other hand, recent results showed that crystalline low molecular weight poly(ethylene oxide) (PEO) complexed with lithium salts exhibits similar or higher ionic conductivity compared to its amorphous counterparts.[30] Despite many efforts, however, the detailed picture of structural properties and the mechanism for ion conduction on a molecular level is still not well understood.

Small-angle neutron scattering (SANS) is a very powerful scattering technique for studies of polymer structures on a molecular level. SANS is particularly useful to probe single chain conformation when performed under dilute conditions where negligible interchain interferences are present or to investigate the polymer melts owing to its longer penetration depth.[31] In any case, only a few polymer electrolyte systems mainly based on PEO salt complexes have been investigated up to now by means of SANS with regard to polymer salt interaction[32−36] or behavior of filler particles in the polymer matrix.[37,38] However thorough investigations of polyphosphazenes in solution and molten state using SANS are, to our knowledge, still missing.

This study intended to perform for the first time neutron scattering experiments on poly(bismethoxyphosphazene) (PBMP) as a model polymer for polyphosphazenes and polyphosphazene-based polymer electrolytes. The methoxy-substituted linear polyphosphazene was chosen, because it can easily be prepared in deuterated form, shows a low T_g value, and has enough polarity for dissolving salts.

* Corresponding author. E-mail hdw@uni-muenster.de. Telephone: +49 251 83 33115. Fax: +49 251 83 33193.
[†] Institut für Anorganische und Analytische Chemie, and SFB 458, Universität Münster.
[‡] Institut für Festkörperforschung, Forschungszentrum Jülich.
[§] International Graduate School of Chemistry (GSC-MS).

10.1021/ma071429e CCC: $40.75
Published on Web 02/28/2008

Besides an investigation of the polyphosphazene molecules in the melt and in diluted solution with a solvent, we also were interested in studying corresponding salt-in-polymer systems and the influence of the dissolved salt on the melt conformation of the polymers as well as their ionic conductivity. The low T_g value was expected to support a good ionic conductivity.

2. Experimental Section

2.1. Materials. All reactions were carried out under an atmosphere of dry nitrogen gas and using standard vacuum-line Schlenk techniques. Pentane (98%, Baker), toluene (99.7%, Scharlau), and 1,4-dioxane (99.5, Grüssing) were distilled from sodium benzophenone ketyl prior to use. Phosphorus trichloride (PCl_3, 99%, Merck) and sulfuryl chloride (SO_2Cl_2, 98%, Merck) were freshly distilled before use. Lithium bis(trimethylsilyl)amide (($LiN(SiCH_3)_2$, 97%, Aldrich), lithium triflate ($LiSO_3CF_3$, purum, Fluka), and phosphorus pentachloride (PCl_5, sublimed under vacuum) were stored under nitrogen in a glovebox. Methanol (purum, Normapur), methanol-d_4 (99.8%, Aldrich) and *N*,*N*-dimethylformamide-d_7 (99.5%, Chemotrade) were used as received. Celite 545 was dried at 120 °C for 48 h before use.

2.2. Equipment. All NMR spectra were measured using a Bruker AC 200, Bruker ARX 300, and a Varian Mercury 400 Plus spectrometer. The spectra were recorded using $CDCl_3$ as the solvent and tetramethylsilane (TMS) as internal reference. For the ^{31}P spectra, 85% H_3PO_4 was used as reference.

The molecular weights and molecular weight distributions (PDI) of the polymer precursors were analyzed by a gel permeation chromatograph, equipped with two PSS−SDV linear XL columns (8 mm × 300 mm, 5μ, Polymer Standards Service, Mainz), a RI-detector (Agilent) and a viscosimeter (η-1001, WGE Dr. Bures). A universal calibration curve performed using polystyrene (Ready-Cal standard, PSS, Mainz) standards was employed for the molecular weight estimation. The flow rate was 0.8 mL/min. As the solvent, tetrahydrofuran (THF) with a 0.1 wt % solution of tetra-*n*-butylammonium bromide was used. The intrinsic viscosity measurement of the polymer was carried out using Schott type Ubbelohde capillary viscometer placed into a water bath at 25 °C controlled by a water regulated thermostat (Thermo Haake). The same solvent composition was employed as GPC measurements. The intrinsic viscosity, [η], and Huggins constant, k_H, were obtained by simultaneous extrapolation of η_{sp}/C to infinite dilution, where η_{sp} is the specific viscosity.

Differential scanning calorimetry (DSC) was used to obtain the glass transition temperatures (T_g) of the polymers. The DSC thermograms were recorded using a Netzsch DSC 204 at a heating rate of 10 K/min under an atmosphere of dry nitrogen.

FT-IR spectra of the polymers, which were pressed between KBr windows, were measured using a Bruker IFS 113v IR or a Shimadzu IRPrestige-21 spectrometer.

Impedance Measurements. The salt-in-polymer electrolytes were prepared by mixing and solvent evaporation from THF solutions of PBMP (**2a**) and the desired amount of lithium triflate (5, 10, 15, and 20 wt %) by a solution casting technique. The attempts to prepare samples with salt concentrations above 20 wt % failed due to insufficient solubility of the salt in the polymer. After solvent evaporation, the samples were kept at least 24 h under vacuum to remove traces of solvent left. The homogeneous samples prepared in this way were sandwiched between two ion blocking stainless steel electrodes separated by a Teflon ring with a diameter of 8 mm and thickness of 1 mm. The whole measurement cell was placed inside a water regulated thermostat (Thermo Haake) and the measurement was carried out under a constant flow of dry nitrogen in a temperature range from 30 to 90 °C. The ionic conductivities of the samples were determined by the impedance data obtained by a Solartron SI 1260 impedance analyzer in a frequency range from 10^6 to 10^{-1} Hz. A predominant ohmic contribution to the impedance, where the phase angle approached to zero, was found at intermediate frequencies from the Cole−Cole plots. This was attributed to the bulk impedance of the polymer electrolyte and used to calculate the ionic conductivities.

Scheme 1. Synthesis of Poly(bismethoxyphosphazene) (PBMP); 2a and 2b

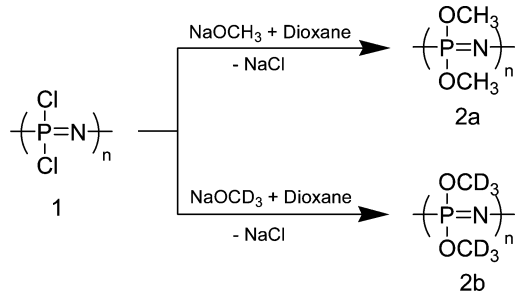

2.3. Synthesis. The synthesis of the monomer trichloro (trimethylsilyl)phosphoranimine ($Cl_3P{=}NSiMe_3$) was carried out according to Wang et al.,[39] with minor modifications.[40] Poly(dichlorophosphazene) was synthesized from this monomer via living cationic polymerization using the route developed by Allcock et al.[41]

The synthesized precursor polymer (**1**) was dissolved in freshly distilled dioxane and divided into two equal portions in order to guarantee identical macromolecular properties for the newly synthesized polymers (cf. **2a** and **2b**, Scheme 1). Instead of synthetic methods based on a large excess of methanol as reported in the literature,[28,29] another approach, as explained below, was used for the introduction of the methoxy groups in the precursor polymer in order to limit the consumption of the deuterated solvent. The final polymer was isolated almost in quantitative yield.

Poly(bismethoxyphosphazene) (PBMP) (2a). A portion of 200 mL of dioxane solution of 10.5 g (90.5 mmol) of poly(dichlorophosphazene) was given slowly to a solution of sodium methoxide, which was prepared previously from metallic sodium (4.58 g, 199.2 mmol) and excess alcohol (6.96 g, 217.3 mmol) in a 500 mL three neck round-bottom flask overnight under reflux. The solution was let to stir at room temperature for 2 days under an inert atmosphere of nitrogen. When the substitution was complete (checked by ^{31}P NMR), the solution was concentrated under vacuum and dialyzed against first in 0.1 M HCl solution for 1 day and then against water for 4 days(dialysis membrane; regenerated cellulose, molecular weight cut off 12000−14000). Finally the water removed by rotary evaporator and dried under high vacuum until constant weight was reached, yielding 9.34 g (96% yield) of slightly yellow highly viscous product. ^1H NMR ($CDCl_3$): $\delta = 3.63$ (broad s). ^{13}C NMR ($CDCl_3$): $\delta = 52.8$. ^{31}P NMR ($CDCl_3$): $\delta = -4.1$. One peak was observed in the GPC measurement with the average molecular weight $M_n = 1.32 \times 10^5$ Da and a polydispersity index (PDI) of 1.22. Elemental analysis wt % calculated (found) for **2a**: C, 22.44 (22.42); H, 5.65 (5.73); N, 13.08 (13.15).

Poly(bis(d_3-methoxy)phosphazene) (d_6-PBMP) (2b). The synthesis and purification of d_6-PBMP was performed using the same reactions conditions described for **2a**. The following reagents and quantities were used: poly(dichlorophosphazene) (10.5 g, 90.5 mmol), sodium (4.58 g, 199.2 mmol), d_3-methanol (7.84 g, 217.3 mmol). The product was 10.03 g (98%) with a slight yellow color. ^1H NMR ($CDCl_3$): no signal. ^{13}C NMR ($CDCl_3$): $\delta = 52.0$. ^{31}P NMR ($CDCl_3$): $\delta = -4.0$. One peak was observed in the GPC measurement with the average molecular weight $M_n = 1.31 \times 10^5$ Da and a polydispersity index (PDI) of 1.23. Anal. Caclcd (found) for **14a**: C, 21.24 (21.19); D, 10.69 (10.74); N, 12.39 (12.22).

2.4. Small-Angle Neutron Scattering (SANS). Sample Preparation. The dilute polymer solutions of PBMP in DMF-d_7 were prepared to study solution characteristics up to 1 vol %. The bulk properties of polymers were investigated for a mixture consisting of 5 vol % PBMP and 95 vol % d_6-PBMP.

The same composition was also used to prepare 5 and 10 mol % $LiSO_3CF_3$ containing solvent free salt-in-polymer electrolytes (corresponding to 7.5 and 15 wt % salt contents respectively). The solutions were contained in Hellma Quartz cells of path lengths of

1 mm. The transmissions were measured in situ from a monitor at $q = 0$ inside the beamstop. The melts have been placed between 2 quartz plates of each 2 mm thickness with a spacer inside keeping the gap between the plates at a value of 1 mm (±5%). The sample aperture for the solutions and melt samples was 10 × 10 mm^2 respectively 8 × 8 mm^2. These cells were put into a brass furnace and the temperature arranged so as to achieve 12.5, 36.6, and 60.6 °C inside the sample using a calibration formula.

Scattering. SANS experiments were performed on the KWS1 spectrometer at the FRJ-2 Dido research reactor in Jülich, Germany. The reactor runs at 20 MW and has a D_2O moderator. The incident wavelength, λ, was 7 Å. Data were collected at distances sample-to-detector of 2, 8, and 20 m, resulting in a q range between 0.002 and 0.2 Å^{-1} in 128 × 128 channels of 5 × 5 mm^2. The scattering vector, q, is the modulus of the resultant between the incident, k_i, and scattered, k_s, wave vectors and related to the scattering angle, θ, as $q = (4\pi/\lambda)\sin(\theta/2)$. The intensities are obtained after appropriate channelwise subtraction of empty cell scattering, background noise due to stray neutrons and γ photons and dark current noise from the electronics. The latter is measured when the beam is blocked with boron carbide. Possible dead time effects are accounted for in the calibration. The absolute differential scattering cross-section or further abbreviated intensity given in cm^{-1} was obtained after calibrating with a 1.5 mm thick secondary standard of Plexiglas which was previously calibrated to vanadium and obtained as

$$\frac{d\Sigma}{d\Omega}(q) = \frac{\left(T_p D_p \frac{d\Sigma_p}{d\Omega}\right) L_S^{\,2}}{T_S T_{EC} D_S L_p^{\,2} \langle I_p \rangle} [(I_S - I_{BC}) - T_S(I_{EC} - I_{BG})] \epsilon_{ij} \quad (1)$$

where subscripts p, S, EC, and BC stand for Plexiglas, sample, empty cell, and boron carbide. The detector sensitivity correction per channel is contained in the ϵ_{ij} matrix and D, T, and L are the thickness, transmission, and detector distance respectively. $d\Sigma_p/d\Omega$ is the known absolute scattering cross section of the standard. Afterward, the 2-dimensional data were radially averaged to yield I vs q and fitted.

3. Results and Discussion

3.1. Characterization of PBMPs. The polymers were synthesized via macromolecular substitution of the precursor poly(dichlorophosphazene) using sodium methoxide. The disappearance of the poly(dichlorophosphazene) signal (−18 ppm) in ^{31}P NMR and new sharp signal observed at around −4.1 ppm, attributed to the target polymers (**2**) were clear indications for the complete substitution and for a high purity of the products. Moreover, the absence of any other signals especially in the range of 5−20 ppm clearly revealed that neither cyclic trimers nor tetramers were produced throughout the synthesis. Here it is worth to mention that the attempts to prepare high quality poly(bismethoxyphosphazenes) in THF were not successful due to concomitant ring-opening polymerization of the solvent to yield poly(tetrahydrofuran) as detected spectroscopically. Therefore, in our case, dioxane was employed as the solvent for the synthesis as it resists ring-opening polymerization.

Both **2a** and **2b** (Scheme 1) showed similar thermal behavior. The T_g values for PBMP and d_6-PBMP were found to be −79.5 and −81.8 °C (the DSC curve of **2a** up to 25 °C is given in Figure 4). The polymer showed no primary transition in the temperature scan range up to around 170 °C, but rearrangement and degradation for both types of polymers were detected above this temperature (not shown in the figure). This corresponds well to the results of former studies concerning the rearrangement and degradation mechanism of the same polyphosphazene.[28,29,42]

Molecular Weight Determination. After the substitution, the molecular weights of the polymers were analyzed by gel permeation chromatography (GPC) using a universal calibration curve. They turned out to be of the order of 10^5 Da for both polymers with almost identical polydispersity index (PDI) values. The weight-average molecular weight of **2a** was estimated as 1.05 × 10^5 Da with a PDI value of 1.43 and 1.04

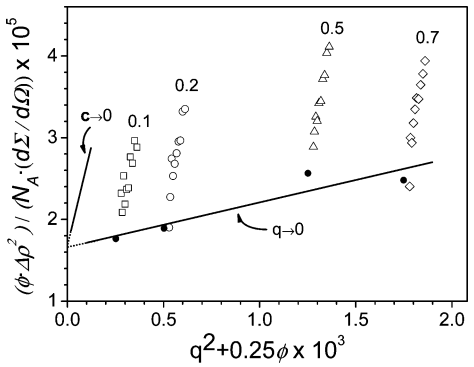

Figure 1. Zimm plot of PBMP prepared in 0.1, 0.2, 0.5, and 0.7 vol % in DMF-d_7. Open symbols are experimental results. Lines are extrapolations as $c \rightarrow 0$ and $q \rightarrow 0$.

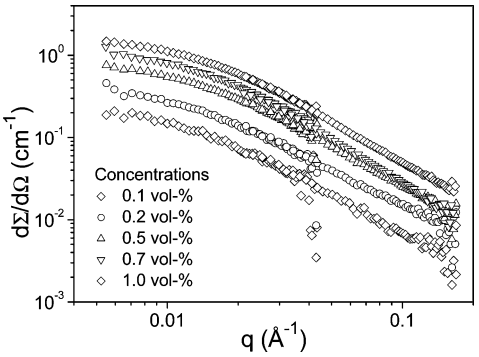

Figure 2. Scattering intensity of polymer solutions as a function of scattering vector. The numbers correspond to volume concentration in DMF-d_7.

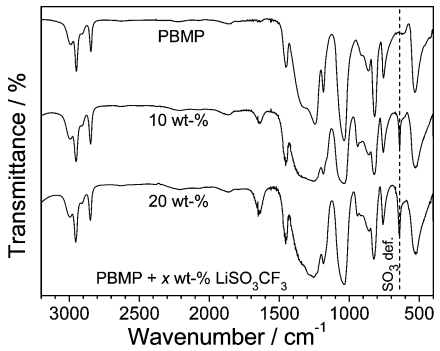

Figure 3. FT-IR spectra of PBMP and its polymer electrolytes for 10 and 20 wt % lithium triflate.

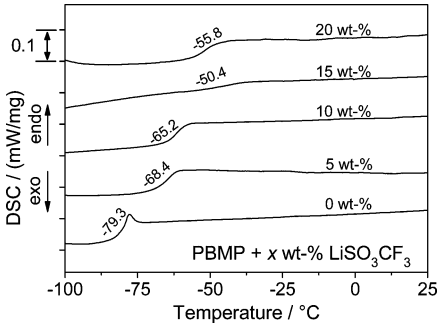

Figure 4. DSC thermogram of pure PBMP and salt-in-PBMP systems with increasing amount of lithium triflate.

$\times 10^5$ Da for **2b** with PDI value of 1.44. The relatively narrow molecular weight distributions indicate that no perceivable degradation or chain cleavage occurred in the course of the macromolecular substitution reaction.

Viscometric measurements yielded an intrinsic viscosity value of 0.51 dL/g with $k_H = 0.55$ for the poly(bismethoxyphosphazene). This value is very similar to that of the polystyrene standard. The Mark−Houwink equation ($[\eta] = KM_v^a$) with $K = 1.17 \times 10^{-4}$ dL/g and $a = 0.725$ as reported by Goeldhart et al.[43] for polystyrene in THF gave almost the same intrinsic viscosity of 0.51 dL/g in this molecular weight range. The product of intrinsic viscosity and the molecular weight is proportional to the hydrodynamic volume of a polymer. Therefore, one can equate the hydrodynamic volumes of our polyphosphazene and the polystyrene standards according to

$$[\eta]_{PBMP} M_{PBMP} = [\eta]_{PS} M_{PS} \quad (2)$$

A comparable intrinsic viscosity value such as found here for poly(bismethoxyphosphazene) was calculated for poly(bisethoxyphosphazene) using reported Mark−Houwink parameters from the literature ($K = 2.5 \times 10^{-4}$ dL/g, $a = 0.46$).[44]

SANS. Dilute solutions of **2** were characterized by SANS using Zimm's extrapolation method, the same method as usually applied for light scattering experiments,[45,46] as depicted in Figure 1, which is a double extrapolation: Letting $c \rightarrow 0$ leads to the single chain limit without interaction and allows the radius of gyration to be extracted. Letting $q \rightarrow 0$ at the same time allows the determination of the forward scattering without effects of interaction because the second virial coefficient A_2 then approaches zero.[45]

In the figure, the *y*-axis is inversely proportional to the structure factor, $S(q)$. ϕ, $\Delta\rho^2/N_A$, and $d\Sigma/d\Omega$ are, respectively, volume fraction of polymer, contrast factor describing the interaction of neutrons and the atoms of the samples and macroscopic differential cross section. The number 0.25 in the *x*-coordinate was chosen arbitrarily to spread the curves horizontally.

Data (crosses) are selected only from the 8 m data, as the lower q (20 m) data were poor statistical quality or showed extra scattering, being non characteristic for the polymer. Only the linear part of the 8 m data in the above representation is used ($0.005 < q < 0.011$ A^{-1}). This range in q allows determining values for R_g of the chains ranging between 90 and 200 Å, i.e. $1/q$, which is appropriate for us.

Besides the R_g value extracted from the Zimm plot, the estimated value of the second virial coefficient A_2 is important as it relates to Flory−Huggins parameter χ which describes the polymer interaction according to

$$2A_2 = \frac{\upsilon_2^2}{V_2}(1 - 2\chi) \quad (3)$$

where υ_2 = specific volume of the polymer and V_2 = partial molar volume of the solvent. A positive, zero, and negative A_2 mean, respectively, a good, a "Θ", or bad solvent according to the general classification.

Using Zimm's approximation, the *z*-average radius of gyration was found to be 144.7 ± 0.2 Å, which at $q = 0$ corresponded to the M_w value of 95000 Da. This value for M_w was slightly lower than the value as determined from GPC. Further, the obtained second virial coefficient A_2 in DMF at room temperature was 8.6×10^{-4} mol·cm^3/g^2, which is of the same order as known from other polymers in a good solvent.

In experimental contexts, Zimm's approximation is preferred when only low q values are available. At higher q values, polymer solutions with excluded volume interactions show a high q behavior proportional to $q^{-1/\nu}$ where ν is the excluded volume exponent, which can be determined from the slope of a logarithmic plot of intensity, I vs q at high q values ($\nu = {}^3/_5$ for fully swollen chains, $\nu = {}^1/_2$ for "Θ" chains, and $\nu = {}^1/_3$ for collapsed chains). Figure 2 shows the scattering intensity of polymer solutions for high q-data (after subtraction of the incoherent background of the solvent = 0.055 cm^{-1}).

The slope was −1.647 and hence in almost exact agreement with the expected excluded volume exponent by Flory, which is ${}^5/_3$, affirming again the good solvent property of this system.

3.2. PBMP-Based Polymer Electrolytes. PBMP was complexed with 5, 10, 15, and 20 wt % lithium triflate and investigated with regard to its conductivity as salt-in-polymer electrolytes. The measurements could only be performed up to 20 wt % salt content due to observed phase separation and precipitation of the salt from the polymer electrolytes above this concentration. The main objective here is to compare the results of neutron scattering experiments with the other thermal and spectroscopic results to have an overall perspective about this model polyphosphazene structure, its interaction with lithium triflate and the electrical properties.

FT-IR. The FT-IR spectrum of salt free PBMP as well as two different salt concentrations is given in Figure 3. The interaction of salt with polyphosphazene by FT-IR spectroscopy can be in principle monitored either by the changes in characteristics stretching modes of possible coordinating sites on the polymer matrix, like O or N atoms, or that for lithium salt, especially the SO_3 group in this case.

Although we expected a certain degree of cation solvation by the oxygen of side groups and the nitrogen of the main chain, the spectra of the polymer electrolytes showed no distinct changes of the intensities and the peak frequencies of the characteristic absorption of P═N at 1450 cm^{-1}, P−O−C at 1185 and 1032 cm^{-1}, and P−O−CH_3 at 821 cm^{-1}. Moreover, a shift to higher frequencies is expected for the SO_2 deformation band at 638 cm^{-1} if additional coordination between oxygen or nitrogen atoms of the polymer and the salt takes place.[40,47] However no change was observed with increasing salt content except a broadening indicating formation of higher ion aggregates.[48] All these findings suggest a rather weak interaction between salt and polymer, and accordingly a polymer-decoupled motion of the salt ions in the solution.

Differential Scanning Chromatography. The glass transition temperatures (T_g) of salt-in-polymer electrolytes were investigated by DSC. They also showed similar thermal behavior as the salt free polymer with very low glass transition temperatures and no additional first-order transitions (Figure 4). The addition of salt depressed the normal decomposition temperature of the polymers from 170 to around 100 °C (not shown in the figure). The T_g values shifted gradually to the higher values as the amount of salt in the polymer electrolyte increased and reached −55.8 °C for 20 wt % salt concentration. This progressive rise is usually attributed to the decrease in the segmental mobility of the polymer, which is usually interpreted as a result of intra- and intermolecular coordinations between coordinating sites and the ions. Although the FT-IR measurements did not reveal considerable salt−polymer interactions, the stiffening as observed from the shift of the T_g values to higher temperatures, indicates at least a minor interaction of the salt with the polymer host.

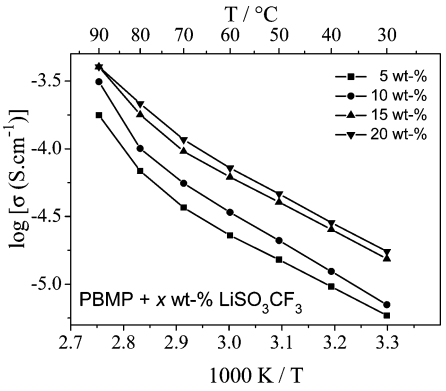

Figure 5. Arrhenius plot for the conductivity of PBMP (**2**) with variable amount of $LiSO_3CF_3$.

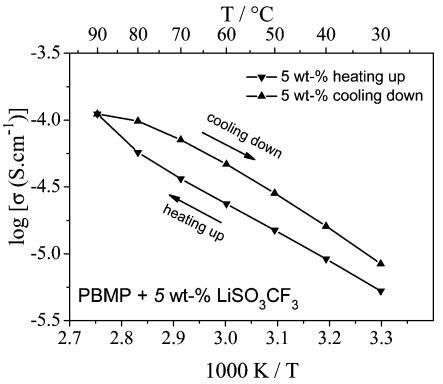

Figure 6. Arrhenius plot for heating and cooling cycle of PBMP with 5 wt % $LiSO_3CF_3$.

***T* and Li-Salt Dependence of Conductivity.** The temperature-dependent ionic conductivity of salt-in-polymer systems was determined using impedance spectroscopy. In order to avoid an influence by the polymer degradation as detected by DSC measurement (taking place at above 90 °C), the first heating and cooling cycle were performed up to 70 °C followed by a last heating up to 90 °C. The temperature dependence of the ionic conductivity is depicted in Figure 5. The investigated system showed a monotonous increase of conductivity with the salt content, but did not show a conductivity maximum in the studied concentration range as often observed in polymer electrolytes. The highest conductivity of 1.7×10^{-5} S/cm was observed for 20 wt % salt containing polymer electrolyte at 30 °C. The conductivity of the polymer electrolytes followed an Arrhenius behavior up to 70 °C as commonly seen for glasses and low molecular weight solvents, indicating that the ion transport was less strongly coupled to the segmental motions of the polymer than usual (Figure 5). The conductivity values unexpectedly deviated from the linearity above 70 °C for all electrolyte systems increasing much faster between 70 and 90 °C. The fairly rapid degradation leading to low molecular weight polymeric or trimeric and tetrameric cyclic organophosphazenes most probably results in a decrease of the overall viscosity of the system.[28,29] In order to reveal the plasticizing effect of these newly formed species, the conductivity of salt-in-polymer electrolyte with 5 wt % lithium triflate was further recorded after the first heating up to 90 °C and cooling-down the system to 30 °C (Figure 6). The distinct increase in the conductivity along the cooling run is clearly seen. This can be well explained by the change in viscosity since the conductivity is inversely related to the viscosity of the solution.

Moreover, it is worth to mention that the room-temperature conductivity of PBMPs was surprisingly high and comparable to the well-known MEEP polymer electrolytes complexed with lithium triflate.[25,26] This is contradictory to the common belief that a polymer should contain solvating groups, such as oligoethers, to establish a high ionic conductivity. These results here indicate that a highly mobile polymer melt with only weak interactions with the dissolved salt ions can also result in rather high conductivities.

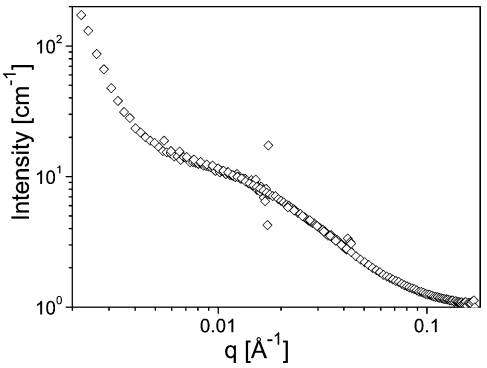

Figure 7. Scattering intensity of polymer blend 5 vol % PBMP + 95 vol % d_6-PBMP as a function of scattering vector at $T = 12.5$ °C.

Polymer and Salt-in-Polymer (in the Molten State). We further applied SANS to the polymer melts and salt-in-polymer electrolytes containing 5 and 10 mol % $LiSO_3CF_3$ relative to the polymer segments (corresponding to approximately 7.5 and 15 wt %).

The blends show considerable parasitic scattering at low q. On the basis of the observed q dependence (which is close to q^{-4}), it can be excluded that this is due to a "simple" isotope mixing effect or Flory−Huggins interaction term between PBMP and d_6-PBMP. It was also present in the salt free samples as well. Therefore, the salt had no distinctive contribution to that. It might be due to much larger structures in the polymer, e.g., in the pre-gel state (i.e., branched structures) or trapped voids in the melt sample. From the ^{31}P NMR analysis, however, we found no evidence for branching and if present, the concentration should be very low. The data show, however, a typical leveling-off in the same way as for the solutions (usable data: $q > 0.007$ Å^{-1}), which can be interpreted as the Guinier plateau of the chain. The Guinier function is simple, and in fact, Zimm's approximation used before is just an expansion of the Guinier function. Figure 7 shows a representative plot for the bulk polymer without salt. The Guinier fitting parameters of the mentioned q range using the following definition are listed in Table 1.

$$\ln(I) = \ln(I_0) - (qR_g)^2/3 \quad (4)$$

Briefly, R_{gz}, which is again the z-average, decreases only a little from 85 Å to 83 Å, if the temperature is increased from 12.5 to 60.6 °C for the polymer melt and remains virtually constant for both salt-in-polymer systems. Although these results showed that the salt exhibited no distinguishable effect on the size of the polymer molecules even with increasing temperature, there must be in fact at least a weak interaction. Otherwise it would not be possible to dissolve lithium triflate up to 20 wt % without any macroscopic phase separation. As seen in the DSC thermograms of the polymer electrolytes (Figure 4), the T_g value is only slightly increased with the addition of salt and the second transition observed (as the salt content increased further) could be attributed to the presence of microheterogeneity with two distinct amorphous microdomains, possibly one salt free and one salt rich. Nevertheless, the overall degree of coordination

Table 1. Guinier Fitting Parameters at $q > 0.007$ Å^{-1} and Evaluations Using Monodisperse Guinier Approach (Yielding R_{gz}) and with a Polydisperse Schulz−Zimm−Flory Distribution (Yielding R_{gn})[a]

name	T (°C)	$\ln(I_0/\text{cm}^{-1})$	Phi*(1-Phi)* V_w* (10^{-20}cm^3)	R_{gz}(Å)	R_{gn}(Å)	B_{gr}	ϵ
polymer melt	12.5	2.68	0.89	85	61.9	0.903	1.01
polymer melt	36.6	2.65	0.84	83.6	60.1	0.931	1.02
polymer melt	60.6	2.62	0.85	83.2	61.9	0.925	1.01
5 mol % salt-in-polymer	12.5	2.55	0.78	84.5	62.0	0.86	1.01
5 mol % salt-in-polymer	36.6	2.54	0.73	84.4	59.4	0.89	1.02
5 mol % salt-in-polymer	60.6	2.53	0.73	85.1	60.6	0.90	1.02
10 mol % salt-in-polymer	12.5	2.41	0.69	83.1	62.0	0.85	1.00
10 mol % salt-in-polymer	36.6	2.41	0.65	84.2	60.5	0.87	1.02
10 mol % salt-in-polymer	60.6	2.39	0.66	84.4	62.5	0.87	1.01

[a] B_{gr} is the incoherent background, which is subtracted and ϵ is the polydispersity index (see text). Average error bars on the extrapolated intensity and R_{gz} are 0.01 and 0.3 respectively. Error bars are 0.3 Å, and 0.01 cm^{-1} on the background. ϵ is of about 5% uncertainty. The temperature is within roughly ±0.5 °C. Phi is the volume fraction of the minority component in the blend (either D or H polymer).

between cations and oxygen or nitrogen atoms of the polymer must be weak. This is also realized from the temperature dependence of the ionic conductivity which suggested a decoupling from segmental motion of the polymer. Any remaining weak cation coordination seems to be rather localized within the polymer matrix so that this did not affect the overall random coil conformation of the almost free polymer chains.

The intensity in the complete q range, however, cannot be simply fitted to a monodisperse Debye-function. This can be recognized already from the slight mismatch of the high "q" slope with −2. Instead, a Schultz−Zimm−Flory (SZF) distribution was used to fit the polydispersity (Table 1).

For monodisperse Gaussian chains, the form factor of the chain $P_{chain}(q,M)$ is expressed by the well-known Debye scattering function

$$P(q) = 2(\exp(-(qR_g)^2) - 1 + (qR_g)^2)/(qR_g)^4 \qquad (5)$$

In the polydisperse case, the radius of gyration, R_g, however, implicitly depends on $W(M)$. Therefore, a correction for polydispersity must be made then by, e.g., inclusion of a Schultz−Zimm−Flory (SZF) distribution:

$$W(M) = \frac{b^{h+1}}{\Gamma(h+1)} M^h \exp(-bM) \qquad (6)$$

with $b = (h + 1)/M_w$, $h = M_n/(M_w - M_n)$ and $M_w/M_n = 1 + \epsilon$.

The radius we obtained from these fittings here is defined as the number-average of R_g. For a SZF distribution, relations for M_w/M_n are known and also for M_z/M_w which is, e.g., $(1 + \epsilon)/(1 + 2\epsilon)$. This leads to

$$R_{gw} = R_{gn}\sqrt{(1 + 2\epsilon)/(1 + \epsilon)} \qquad (7)$$

The fitted polydispersity (PDI $= 1 + \epsilon = 2.01$) was larger than the GPC result, which was around 1.43. An average M_w of 120000 Da was calculated from the forward scattering at $q = 0$ from fits with the Schultz−Zimm−Flory distribution, which corresponds to a M_n of 60400 Da using the obtained polydispersity. This result was in really good agreement with the value extracted from the experiment done on polymer solutions in DMF-d_7, for which a value of 64000 Da was estimated for M_n. These exact absolute molecular weight results as measured by the SANS experiment were slightly different from the relative molecular weights determined by GPC using polystyrene standards. The M_w value from GPC was 105000 Da with a PDI of 1.43, which corresponds to the M_n value of 73000 Da, indicating a slight deviation from the SANS results.

4. Conclusions

For the first time, SANS was applied to a linear polyphosphazene. Average M_w values from GPC were well comparable to values acquired by the SANS experiments, the difference being not significant. The comparison shows that the molecular weight was only slightly different from the GPC result for M_w.

On the other hand, the influence of the dissolved salt on the melt conformation of the polyphosphazene was investigated. The main result was that the salt-in-PBMP solutions virtually showed no significant effect on the R_g values as compared to pure polymer melts indicating a rather weak interaction between salt and polymer itself. The FT-IR and impedance measurements were also in agreement with these SANS results indicating a predominance of ion pairs and their coupled transport within the polyphosphazene. This is furthermore in agreement with recent results on the role of ion pairs in ion transport of polymer electrolytes.[49−51] Of course, one cannot exclude the presence and contribution of higher ion clusters besides ion pairs.

Despite the weak interaction between polymer and salt, the ionic conductivity was rather high and comparable to that of MEEP-based polymer electrolytes. These results show that the presence of a polymer with high segment mobility is the predominating factor for salt diffusion and conductivity.

References and Notes

(1) Allcock, H. R. In *Synthesis and Characterizations of Poly(organophosphazenes)*; Gleria, M., de Jaeger, R., Eds.; Nova Science Publishers: New York, 2004; pp 49−67.
(2) Wisian-Neilson, P. In *Synthesis and Characterizations of Poly(organophosphazenes*), Gleria, M.; de Jaeger, R., Eds.; Wisian-Neilson: New York, 2004; pp 109−123.
(3) Gleria, M.; De Jaeger, R. In *New Aspects in Phosphorus Chemistry V*; Majoral, J.-P., Ed.; Springer: Berlin, 2005; Vol. 250, pp 165−251.
(4) Pintauro, P. N.; Wycisk, R. In *Phosphazenes*; Gleria, M., de Jaeger, R., Eds.; Nova Science Publishers: New York, 2004; pp 591−620.
(5) Hickner, M. A.; Ghassemi, H.; Kim, Y. S.; Einsla, B. R.; McGrath, J. E. *Chem. Rev.* **2004**, *104*, 4587−4611.
(6) Pintauro, P. N.; Wycisk, R. In *Applicative Aspects of Poly(organophosphazenes*); Gleria, M., de Jaeger, R., Eds. Nova Science Publishers: New York, 2004; pp 225−254.
(7) Allcock, H. R.; Wood, R. M. *J. Polym. Sci., Part B: Polym. Phys.* **2006**, *44*, 2358−2368.
(8) Inoue, K. In *Phosphazenes*, Gleria, M.; de Jaeger, R., Eds. Nova Science Publishers: New York, 2004; pp 535−554.
(9) Allcock, H. R.; Welna, D. T.; Stone, D. A.; Powell, E.; Wood, R. M.; Chang, Y.; Kwak, G. *PMSE Prepr.* **2005**, *93*, 782.
(10) Laurencin, C. T.; Ambrosio, A. M. A. In *Biodegradable Polymers*; Arshady, R., Ed.; Citus Books: London, 2003; Vol. 2, pp 153−173.
(11) Heyde, M.; Schacht, E. In *Applicative Aspects of Poly(organophosphazenes)*; Gleria, M., de Jaeger, R., Eds.; Nova Science Publishers: New York, 2004; pp 1−32.

(12) Laurencin, C. T.; Nair, L. S. In *NATO Science Series, II: Mathematics, Physics and Chemistry*; Guceri, S., Gogotsi, Y. G., Kuznetsov, V., Eds.; Kluwer Academic Publishers: Dordrecht, The Netherlands, 2004; Vol. 169, pp 283−302.
(13) Carenza, M.; Lora, S.; Fambri, L. In *Biomaterials: From Molecules to Engineered Tissues*; Hasirci, N., Hasirci, V., Eds.; Kluwer Academic/Plenum Publishers: New York, 2004; Vol. 553, pp 113−122.
(14) Andrianov, A. K. *Polym. Prepr. (Am. Chem. Soc., Div. Polym. Chem.)* **2005**, *46* (2), 715.
(15) Nair, L. S.; Lee, D.; Laurencin, C. T. In *Handbook of Biodegradable Polymeric Materials and Their Applications*; Mallapragada, S. K., Narasimhan, B., Eds.; American Scientific Publishers: Los Angeles, 2006; Vol. 1, pp 277−306.
(16) Nair, L. S.; Khan, Y. M.; Laurencin, C. T. In *Introduction to Biomaterials*; Guelcher, S. A., Hollinger, J. O., Eds. CRC Press: Boca Raton, FL, 2006; pp 273−290.
(17) Golemme, G.; Drioli, E. In *Applicative Aspects of Poly(organophosphazenes)*; de Jaeger, R., Gleria, M., Eds.; Nova Science Publishers: New York, 2004; pp 555−572.
(18) Golemme, G.; Drioli, E. In *Applicative Aspects of Poly(organophosphazenes)*; Gleria, M., de Jaeger, R., Eds.; Nova Science Publishers: New York, 2004; pp 189−206.
(19) Stewart, F. F.; Luther, T. A.; Harrup, M. K.; Orme, C. J. In *Phosphazenes*; Gleria, M., de Jaeger, R., Eds.; Nova Science Publishers: New York, 2004; pp 573−590.
(20) Stewart, F. F.; Luther, T. A.; Harrup, M. K.; Orme, C. J. In *Applicative Aspects of Poly(organophosphazenes)*; Gleria, M., de Jaeger, R., Eds.; Nova Science Publishers: New York, 2004; pp 207−224.
(21) Allen, C. W.; Hernandez-Rubio, D. In *Applicative Aspects of Poly-(organophosphazenes)*; Gleria, M., de Jaeger, R., Eds.; Nova Science Publishers: New York, 2004; pp 119−137.
(22) Allen, C. W.; Hernandez-Rubio, D. In *Phosphazenes*; Gleria, M., de Jaeger, R., Eds.; Nova Science Publishers: New York, 2004; pp 485−503.
(23) Gray, F. M. *Solid Polymer Electrolytes: Fundamentals and Technological Applications*; John Wiley & Sons: New York, 1991.
(24) Gray, F. M. *Polymer Electrolytes*; The Royal Society of Chemistry: Cambridge, U.K., 1997.
(25) Blonsky, P. M.; Shriver, D. F.; Austin, P.; Allcock, H. R. *J. Am. Chem. Soc.* **1984**, *106*, 6854−6855.
(26) Blonsky, P. M.; Shriver, D. F.; Austin, P.; Allcock, H. R. *Solid State Ionics* **1986**, *18*−*19*, 258−264.
(27) Allcock, H. R.; Austin, P. E.; Neenan, T. X.; Sisko, J. T.; Blonsky, P. M.; Shriver, D. F. *Macromolecules* **1986**, *19*, 1508−1512.
(28) Allcock, H. R.; Kugel, R. L.; Valan, K. J. *Inorg. Chem.* **1966**, *5*, 1709−1715.
(29) Mochel, V. D.; Cheng, T. C. *Macromolecules* **1978**, *11*, 176−179.
(30) Christie, A. M.; Lilley, S. J.; Staunton, E.; Andreev, Y. G.; Bruce, P. G. *Nature (London)* **2005**, *433* (7021), 50−53.
(31) Higgins, J. S.; Benoit, H. C. *Polymers and Neutron Scattering*. Clarendon Press: Oxford, U.K., 1994.
(32) Hakem, I. F.; Lal, J. *Appl. Phys. A: Mater. Sci. Process.* **2002**, *74*, S531−S533.
(33) Hakem, I. F.; Lal, J. *Europhys. Lett.* **2003**, *64* (2), 204−210.
(34) Hakem, I. F.; Lal, J.; Bockstaller, M. R. *Macromolecules* **2004**, *37*, 8431−8440.
(35) Annis, B. K.; Badyal, Y. S.; Simonson, J. M. *J. Phys. Chem. B* **2004**, *108*, 2554−2556.
(36) Hakem, I. F.; Lal, J.; Bockstaller, M. R. *J. Polym. Sci., Part B: Polym. Phys.* **2006**, *44*, 3642−3650.
(37) Karlsson, C.; Best, A. S.; Swenson, J.; Kohlbrecher, J.; Borjesson, L. *Macromolecules* **2005**, *38*, 6666−6671.
(38) Qiu, D.; Cosgrove, T.; Howe, A. M. *Langmuir* **2006**, *22*, 6060−6067.
(39) Wang, B.; Rivard, E.; Manners, I. *Inorg. Chem.* **2002**, *41*, 1690−1691.
(40) Paulsdorf, J.; Kaskhedikar, N.; Burjanadze, M.; Obeidi, S.; Stolwijk, N. A.; Wilmer, D.; Wiemhöfer, H. D. *Chem. Mater.* **2006**, *18*, 1281−1288.
(41) Allcock, H. R.; Reeves, S. D.; de Denus, C. R.; Crane, C. K. *Macromolecules* **2001**, *34*, 748−754.
(42) Allcock, H. R. *Chemistry and Applications of Polyphosphazenes*; John Wiley & Sons: Hoboken, NJ, 2003.
(43) Goedhart, D.; Opschoor, A. *J. Polym. Sci., Part A2* **1970**, *8*, 1227−1233.
(44) Tarazona, M. P.; Bravo, J.; Rodrigo, M. M.; Saiz, E. *Polym. Bull. (Berlin)* **1991**, *26*, 465−471.
(45) Dhont, J. K. G.; Gompper, G.; Richter, D. *Soft Matter: Complex Materials on Mesoscopic Scales*; Forschungszentrum Jülich GmbH: Jülich, Germany, 2002.
(46) Büeckel, T.; Heger, G.; Richter, D.; Zorn, R. *Laboratory Course Neutron Scattering*; Forschungszentrum Jülich GmbH: Jülich, Germany, 2005.
(47) Luther, T. A.; Stewart, F. F.; Budzien, J. L.; LaViolette, R. A.; Bauer, W. F.; Harrup, M. K.; Allen, C. W.; Elayan, A. *J. Phys. Chem. B* **2003**, *107*, 3168−3176.
(48) Fernandez, L. E.; BenAltabef, A.; Varetti, E. L. *Spectrochim. Acta. A. Mol. Biomol. Spectrosc.* **1996**, *52*, 287−296.
(49) Pas, S. J.; Banhatti, R. D.; Funke, K. *Solid State Ionics* **2006**, *177*, 3135−3139.
(50) Stolwijk, N. A.; Wiencierz, M.; Obeidi, S. *Faraday Discuss.* **2007**, *134*, 157−169.
(51) Obeidi, S.; Stolwijk, N. A. *J. Phys. Chem. B* **2006**, *110*, 22496−22502.

MA071429E